



## Corrosion Inhibition of Zinc Using Some Phenylthiazole Derivatives in Hydrochloric acid Solutions

A.S. Fouda<sup>\*a</sup>, A. Abdel Nazeer<sup>b</sup>, K.M. AbdelKhalek<sup>a</sup>

<sup>a</sup>Department of Chemistry, Faculty of Science, El-Mansoura University, El-Mansoura-35516, Egypt.

E-mail: [asfouda@mans.edu.eg](mailto:asfouda@mans.edu.eg),

<sup>b</sup>Electrochemistry and Corrosion Lab., National Research Centre, Dokki, Cairo-12622, Egypt.

### ABSTRACT

The inhibitive action of some phenylthiazole derivatives namely: 2-acetylamino-5-p-bromophenylazo-4-phenylthiazole (BPT), 2-acetylamino-5-p-methylphenylazo-4-phenylthiazole (MPT), 2-acetylamino-5-p-methoxyphenylazo-4-phenylthiazole (XPT) and 2-acetylamino-5-p-nitrophenylazo-4-phenylthiazole (NPT), on zinc corrosion in 0.2 M HCl has been studied using weight loss, potentiodynamic polarization, electrochemical impedance spectroscopy (EIS) and electrochemical frequency modulation (EFM) measurements. The results showed that the dissolution rate of zinc decreases with increasing the phenylthiazole derivatives concentration and decreases with raising temperature. Polarization curves indicated that the studied inhibitors act as mixed-type inhibitors. The adsorption of the investigated compounds follows Langmuir adsorption isotherm model. The thermodynamic parameters of adsorption and corrosion processes were determined and discussed.

**Keywords:** Acid corrosion; Zinc; Phenylthiazole derivatives; EIS; EFM.



## Council for Innovative Research

Peer Review Research Publishing System

**Journal:** Journal of Advances in Chemistry

Vol. 4, No. 2

[editor@cirworld.com](mailto:editor@cirworld.com)

[www.cirworld.com](http://www.cirworld.com), [member.cirworld.com](http://member.cirworld.com)

## 1. Introduction

Zinc is one of the most widely used metal and is often attacked by aggressive media such as acids, bases and salt solutions [1-2]. Acids are widely used in industries such as pickling, cleaning, descaling [3-5]. In a pickling process, strong acid solutions not only remove the fouling and rust on the metal surface, but they also react with the base metal and consume excessive metal materials. As a traditional technique of surface treatment, acid pickling is a heavily polluting process due to its release and discharge of significant amounts of acid fogs and spent pickling liquors, respectively. So far, however, there is no alternative method to totally replace it for the surface treatment of iron and steel materials [6].

In efforts to mitigate electrochemical corrosion, the strategy is to isolate the metal from corrosive agents. Use of corrosion inhibitors is the most economical and practical method to achieve this objective. Actually, most mechanisms of corrosion inhibition are the formation of a protective film at the metal-solution interface either by adsorption or deposition. Up to now, organic compounds containing N, P, S, and O in their molecular structures have been confirmed to be effective inhibitors because of their ability to be adsorbed on the metal surface. Adsorption of these compounds on the metal surface leading to the formation of a protective film [7-10], due to the interaction of the lone pair electron and/or  $\pi$ -orbitals of the inhibitor with the d-orbitals of the metal surface atoms, and is highly dependent on the nature and surface charge of the metal, the type of aggressive electrolyte, and the chemical structure of the inhibitor [11]. The action of inhibition of zinc in acidic media by various organic and inorganic inhibitors has been widely investigated by many authors [12-26].

In the present work, we investigated the effect of some phenylthiazole derivatives on the electrochemical behavior of zinc in acidic medium using chemical (weight loss) and electrochemical measurements (potentiodynamic polarization, electrochemical impedance spectroscopy (EIS) and electrochemical frequency modulation (EFM)) techniques.

## 2. Experimental

Experiments were performed using zinc sheet with the following composition (weight %): 0.003 Cu, 0.002 Fe, 0.001 Pb, 0.001 Cd and the rest Zn. The aggressive solution used was made of analytical reagent grade HCl. Appropriate concentration of acid was prepared using double distilled water.  $10^{-3}$ M stock solution from the investigated compounds was prepared by dissolving the appropriate weight in double distilled water.

- Structures, names, molecular formulae, and molecular weights of the investigated phenylthiazole derivatives are:

Comp.	Structures	Names	M. FW. & M. Wt.
BPT		2-acetylamino-5-p-bromophenylazo-4-phenyl thiazole	$C_{17}H_{13}BrN_4OS$ 401.28
MPT		2-acetylamino-5-p-methylphenylazo-4-phenylthiazole	$C_{18}H_{16}N_4OS$ 336.41

XPT		2-acetylamino-5-p-methoxyphenylazo -4-phenylthiazole	$C_{18}H_{16}N_4O_2S$ 352.41
NPT		2-acetylamino-5-p-nitrophenylazo -4-phenylthiazole	$C_{17}H_{13}N_5O_3S$ 367.38

For weight loss measurements, rectangular zinc specimens of size 20 x 20 x 2 mm were immersed in 100 ml inhibited and uninhibited solutions and allow to stand for several intervals at 25 °C in water thermostat. The percentage inhibition efficiency (% I) and the degree of surface coverage ( $\theta$ ) of the investigated compounds were calculated from equation (1):

$$\% I = \theta \times 100 = [1 - (M_{inh} / M_{free})] \times 100 \quad (1)$$

where  $M_{free}$  and  $M_{inh}$  are the weight losses per unit area in the absence and presence of the investigated compounds, respectively.

All electrochemical experiments were carried out in a conventional three-electrode cell with platinum foil 1 cm<sup>2</sup> as counter electrode, a saturated calomel electrode as a reference electrode and zinc sheet (1 x 1 cm) embedded in epoxy resin of polytetrafluoroethylene as a working electrode. Before polarization, working electrode was immersed in the test solution for 30 minute until steady state potential was attained. Measurements were performed in the 0.2 M HCl solution containing different concentrations of the investigated inhibitors by changing the electrode potential automatically from -1.5 to -0.25 V at scan rate of 0.5 mV s<sup>-1</sup>. The linear Tafel segments of anodic and cathodic curves were extrapolated to corrosion potential to obtain corrosion current densities ( $i_{corr}$ ). The inhibition efficiency (% I) and the degrees of surface coverage ( $\theta$ ) were defined as [27]:

$$\% I = \theta \times 100 = [(i_{corr} - i_{corr}^0) / i_{corr}^0] \times 100 \quad (2)$$

where  $i_{corr}$  and  $i_{corr}^0$  are the uninhibited and inhibited corrosion current density values, respectively, determined by extrapolation of Tafel lines to the corrosion potential.

Electrochemical frequency modulation (EFM) technique is a nondestructive technique that can directly and rapidly gives values of the corrosion current without a prior knowledge of Tafel constants. EFM data have been analyzed using Echem analyst 5.21. In this work, potential perturbation signal with amplitude of 10 mV with two sine waves of 2 and 5 Hz was applied. The intermodulation spectra containing current responses were assigned for harmonical and intermodulation current peaks. The larger peaks were used to calculate the corrosion current density ( $i_{corr}$ ), the Tafel constants ( $\beta_c$  and  $\beta_a$ ) and the causality factors CF-2 and CF-3.

The EIS spectra were recorded at open circuit potential (OCP) after immersion the electrode for 30 minutes in the test solution. The AC signal was 5 mV peak to peak and the frequency range studied was between 100 kHz and 0.2 Hz.

All experiments were carried out using Potentiostat/Galvanostat/Zra analyzer (Gamry PCI300/4). A personal computer with DC105 software for polarization, EIS300 software for EIS and EFM140 software for EFM measurements and Echem analyst 5.21 was used for data fitting and calculating. The inhibition efficiency (% I) and the surface coverage ( $\theta$ ) of the investigated inhibitors obtained from the impedance measurements can be calculated by applying Eq. (3):

$$\% I = \theta \times 100 = [(R_{ct} - R_{ct}^0) / R_{ct}] \times 100 \quad (3)$$

where  $R_{ct}^0$  and  $R_{ct}$  are the charge transfer resistance in the absence and presence of inhibitor, respectively.



### 3. Results and discussion

#### 3.1. Weight-loss measurements

Weight loss of zinc was determined at various time intervals in the absence and presence of different concentrations of four phenylthiazole derivatives. Figure (1) shows the effect of increasing concentration of BPT, the least effective one, on the weight loss of zinc vs. time curves at 25 °C. Similar curves were obtained for other compounds (not shown). From this Figure, it is obvious that the weight loss of zinc in the presence of BPT varies linearly with time, and is much lower than that obtained in acid solution alone. The linearity obtained indicated the absence of insoluble surface film during corrosion and that the inhibitors were first adsorbed onto the metal surface and therefore, impede the corrosion process [28]. In the absence of inhibitor, the metal dissolution occurs due to the attack of the aggressive ions to the metal surface but at low concentration of the inhibitor, the dissolution of the metal ions decreases due to the adsorption of inhibitor molecules on the zinc surface. At high inhibitor concentration a compact and coherent film of the inhibitor is formed on the zinc surface which reduces the metal attacks. The inhibition efficiency increases in the following order (Table 1): BPT < MPT < XPT < NPT

##### 3.1.1 Adsorption isotherm

Various adsorption isotherms were applied to fit  $\theta$  values and the best fit was found to obey Langmuir adsorption isotherm [29] which may be expressed by:

$$C/\theta = 1/K_{ads} + C \quad (4)$$

where C is the inhibitor concentration and  $K_{ads}$  is equilibrium constant of adsorption. It is well known that the standard free energy of adsorption ( $\Delta G^{\circ}_{ads}$ ) is related to  $K_{ads}$  and  $\Delta G^{\circ}_{ads}$  can be calculated by the following equation [30]:

$$K_{ads} = 1/55.5 \exp [-\Delta G^{\circ}_{ads}/RT] \quad (5)$$

The value of 55.5 represents the molar concentration of water in mol L<sup>-1</sup>. Straight lines were obtained by plotting C/ $\theta$  vs. C showing a very good agreement between the Langmuir isotherm and experimental data ( $R^2 > 0.999$ ) with slope is close to the theoretical value of one (Figure 2). The validity of Langmuir's isotherm of adsorption of the investigated phenylthiazole derivatives on zinc indicates that the interaction forces between the molecules in the adsorbed layer are equal to zero. A value of -40 kJ mol<sup>-1</sup> is usually adopted as a threshold value between chemical and physical adsorption [31]. The calculated values of  $\Delta G^{\circ}_{ads}$ , for the investigated phenylthiazole derivatives are equal to -39.7, -35.5, -31.2 and -29.5 kJ mol<sup>-1</sup> for NPT, XPT, MPT, and BPT, respectively, indicating both physical and chemical adsorption [32]. Also, it is found that the kinetic-thermodynamic model of El-Awady et al [33].

$$\log (\theta / 1 - \theta) = \log k' + y \log C \quad (6)$$

is fitted well the present adsorption data.  $K_{ads} = K' (1/y)$ , K' is constant and 1/y is the number of the surface active sites occupied by one inhibitor molecule and C is the bulk concentration of the inhibitor. Plotting log ( $\theta/1-\theta$ ) against log C for the investigated compounds are given in Figure 3, where straight-line relationship was obtained suggesting the validity of this model for the studied compounds. The values of  $K_{ads}$  and  $\Delta G^{\circ}_{ads}$  calculated from Langmuir isotherm and 1/y,  $K_{ads}$  and  $\Delta G^{\circ}_{ads}$  calculated from the kinetic model are given in Table 2. The negative values of  $\Delta G^{\circ}_{ads}$  suggest that the adsorption of these compounds onto zinc surface is a spontaneous process. It is obvious that the value of 1/y is more than unity suggesting that phenylthiazole derivatives molecules will form monolayer on the zinc surface. In general the values of  $\Delta G^{\circ}_{ads}$  obtained from El-Awady et al. model were comparable with that obtained from Langmuir isotherm. It should be mentioned that the higher values of  $K_{ads}$  and  $\Delta G^{\circ}_{ads}$  refer to a higher adsorptive and thus a higher inhibiting effect [34].

##### 3.1.2 Effect of temperature

The effect of temperature on the corrosion rate of zinc in 0.2 M HCl over the temperature range (30-50°C) in the absence and presence of different concentrations of the investigated compounds has been studied. The inhibition efficiency was found to decrease with increasing the temperature; this may be attributed to increase in the solubility of the protective films and of any reaction products precipitated on the surface of the metal that may otherwise inhibit the reaction rate. As reported before [35], a decrease in the inhibition efficiency with increasing temperature indicates the physisorption of the inhibitors on the corroding metal surface while the reverse behavior implies chemisorptions. Similar observations have been reported elsewhere [36, 37]. Plots of logarithm of corrosion rate (log k), with reciprocal of absolute temperature (1/T) for zinc in 0.2 M HCl at different concentrations of PT after 120 min. are shown in (Figure 4). As shown from this Figure, straight lines with slope of  $-E_a^{\ddagger} / 2.303R$  and intercept of A were obtained according to Arrhenius-type equation (7):

$$k = A \exp (-E_a^{\ddagger} / RT) \quad (7)$$

where: k is the corrosion rate, A is a constant depends on a metal type and electrolyte, and  $E_a^{\ddagger}$  is the apparent activation energy. Plots of log (corrosion rate/ T) vs. 1/ T for zinc in 0.2 M HCl at different concentrations of BPT are shown in (Figure 5). As shown from this Figure, straight lines with slope of  $(-\Delta H^{\ddagger} / 2.303R)$  and intercept of  $(\log R / Nh + \Delta S^{\ddagger} / 2.303R)$  were obtained according to transition state equation (8):

$$\text{Rate} = RT / Nh \exp (\Delta S^{\ddagger} / R) \exp (-\Delta H^{\ddagger} / RT) \quad (8)$$

where h is Planck's constant, N is Avogadro's number,  $\Delta H^{\ddagger}$  is the activation enthalpy and  $\Delta S^{\ddagger}$  is the activation entropy. The calculated values of the apparent activation energy,  $E_a^{\ddagger}$ , activation enthalpies,  $\Delta H^{\ddagger}$  and activation entropies,  $\Delta S^{\ddagger}$  are



given in Table 6. These values indicate that the presence of inhibitors increases  $E_a^*$  and  $\Delta H^*$  and decreases  $\Delta S^*$  for the corrosion process. The increase in  $E_a^*$  indicating a strong adsorption of inhibitor molecules on zinc surface and indicates the energy barrier caused by the adsorption of inhibitors on zinc surface. The increase in  $\Delta H^*$  in presence of inhibitor implies that the addition of inhibitor to the acid solution increases the height of the energy barrier of the corrosion reaction to an extent depends on the type and concentration of the inhibitor. The entropy of activation ( $\Delta S^*$ ) values in the absence and presence of inhibitor are large and negative indicating that the activated complex represents association rather than dissociation step, meaning that a decrease in disordering takes place on going from reactants to the activated complex and the activated molecules were in higher order state than that at the initial state [38-40].

### 3.2. Potentiodynamic polarization measurements

The values of corrosion potential ( $E_{corr}$ ), corrosion current density ( $i_{corr}$ ), and anodic and cathodic Tafel slopes ( $\beta_a$  and  $\beta_c$ ) can be evaluated from anodic and cathodic regions of Tafel plots. The linear Tafel segments of anodic and cathodic curves were extrapolated to corrosion potential to obtain corrosion current densities. The inhibition efficiency (% I), and the surface coverage,  $\theta$ , were evaluated from the measured ( $i_{corr}$ ) values using equation (3). Potentiodynamic polarization curves for the corrosion of zinc in 0.2 M HCl in the absence and presence of different concentrations of BPT are presented in Figure 6. Similar curves were obtained for MPT, XPT and NPT (not shown). From this Figure, it is obvious that both the cathodic and anodic reactions are inhibited and the inhibition increases as the inhibitor concentration increases, but the cathode is more polarized. The values of various electrochemical parameters derived from Tafel polarization of all inhibitors are given in Table 4. From this Table it is clear that, there is no definite trend observed in the  $E_{corr}$  values in the presence of investigated compounds. In the present study, shift in  $E_{corr}$  values is in the range of 40 mV suggesting that all inhibitors act as mixed type [41]. Also, the change in  $\beta_a$  and  $\beta_c$  values indicates that adsorption of investigated compounds affect the mechanism of anodic dissolution as well as cathodic hydrogen evolution. This, confirm that these investigated compounds act as mixed type inhibitors [42]. It is seen (Table 4) that the inhibition efficiency of the phenylthiazole derivatives is in the following order: BPT < MPT < XPT < NPT. Increase in the inhibition efficiency with increasing concentration of all investigated phenylthiazole derivatives studied reveals that the inhibition action are due to adsorption of these inhibitors on zinc surface.

### 3.2 Electrochemical impedance spectroscopy (EIS)

The corrosion behavior of zinc in 0.2 M HCl solution in the absence and presence of different concentrations of the investigated phenylthiazole derivatives was investigated by the EIS method at 25°C. Figure 7 shows the Nyquist plots for zinc in 0.2 M HCl solution in the absence and presence of different concentrations of BPT at 30°C. Similar curves were obtained for other phenylthiazole derivatives (not shown). It follows from this Figure that a depressed charge-transfer semicircle was observed. This semicircle is attributed to the time constant of charge-transfer and double-layer capacitance [43-45]. An equivalent circuit was proposed to represent the corrosion of zinc in 0.2 M HCl solution as shown in Figure 8, where  $R_s$  is the solution resistance,  $R_{ct}$  is the charge transfer resistance,  $C_{dl}$  is the double-layer capacitance. One constant phase element (CPE) is substituted for the capacitive element to give a more accurate fit [46], as the obtained capacitive loop is depressed semicircle rather than regular one.

The surface coverage ( $\theta$ ) and the inhibition efficiencies (% I) were calculated from Eq. (4). The associated parameters with the impedance diagrams are given in Table (5). From the impedance results we found that as the inhibitor concentration increased,  $R_{ct}$  values increased, but  $C_{dl}$  values tended to decrease. The decrease in  $C_{dl}$ , which can result from a decrease in local dielectric constant and/or an increase in the thickness of the electrical double layer, suggests that the investigated phenylthiazole derivatives function by adsorption at the metal/solution interface [47]. The change in  $R_{ct}$  and  $C_{dl}$  values was caused by the gradual replacement of water molecules by the anions of  $Cl^-$  and adsorption of the organic molecules on the metal surface, reducing the extent of dissolution [48]. The order of inhibition efficiency obtained from EIS measurements increases as follows: BPT < MPT < XPT < NPT. The inhibition efficiencies calculated from impedance data are very close to those obtained from potentiodynamic polarization measurements. The results show good agreement between the measurements obtained from both techniques.

### 3.3. Electrochemical frequency modulation (EFM)

Electrochemical frequency modulation technique is a non-destructive corrosion measurement technique that can directly give values of the corrosion current without prior knowledge of Tafel constants [48, 49]. Because current is a non-linear function of potential excitation. The current response contains not only the input frequencies, but also contains frequency components which are the sum, difference, and multiples of the two input frequencies. Figure 9 shows the intermodulation spectra obtained from EFM measurements of zinc in 0.2 M HCl in the presence of different concentrations of BPT. Similar curves were obtained for other phenylthiazole derivatives (not shown). Each spectrum is a current response as a function of frequency. Table 6 shows the corrosion kinetic parameters such as inhibition efficiency (% I), corrosion current density  $i_{corr}$ , Tafel constants ( $\beta_a$ ,  $\beta_c$ ) and causality factors (CF-2, CF-3) as a function of inhibitor concentration. It is obvious from this Table that  $i_{corr}$  values decrease, while those of % I increase with increasing the inhibitor concentration. The great strength of the EFM is the causality factors which serve as an internal check on the validity of the EFM measurement [50]. With the causality factors the experimental EFM data can be verified. The causality factors in Table 6, which are compatible with the theoretical values according to the EFM theory [51], should guarantee the validity of Tafel slopes and corrosion current densities. The standard values for CF-2 and CF-3 are 2.0 and 3.0, respectively. It is quite obvious that the data obtained from polarization and impedance measurements were in good agreement with the results obtained from EFM.



### 3.4. Mechanism of inhibition

The inhibition action of the investigated phenylthiazole derivatives towards the corrosion of zinc in 0.2 M HCl could be attributed to several factors including the structure, the number and types of adsorption sites, the nature of molecules, the metal surface, and the ability to form complexes [52]. The adsorption of investigated compounds can be attributed to the presence of polar unit having atoms of nitrogen, sulphur and oxygen and aromatic/heterocyclic rings. Therefore, the possible reaction centers are unshared electron pair of hetero-atoms and  $\pi$ -electrons of aromatic ring [53]. The adsorption and inhibition effect of investigated compounds in 0.2 M HCl solution can be explained as follows: In aqueous acidic solutions, the phenylthiazole derivatives exist either as neutral molecules or as protonated molecules and may adsorb on the metal/acid solution interface by one and/or more of the following ways: (i) electrostatic interaction of protonated molecules with already adsorbed chloride ions, (ii) donor-acceptor interactions between the  $\pi$ -electrons of aromatic ring and vacant d orbital of surface iron atoms, (iii) interaction between unshared electron pairs of hetero-atoms and vacant d-orbital of zinc surface atoms. Since it is well known that the zinc surface bears the negative charge in acidic solutions [54], so it is easy for the protonated molecules to approach the negatively charged zinc surface ( $H_3O/metal$  interface) due to electrostatic attraction. Thus we can conclude that inhibition of zinc corrosion in 0.2 M HCl is mainly due to electrostatic interaction. The decrease in inhibition efficiency with rise in temperature supports electrostatic interaction.

The order of decreasing the inhibition efficiency of the investigated compounds in 0.2 M HCl solution is as follows: BPT < MPT < XPT < NPT, this behavior can be rationalized on the basis of the structure-corrosion inhibition relationship of organic compounds. Compound NPT is the most effective one, due to the presence of nine adsorption centers (5-N, 3-O and one S atom). Compound XPT comes after compound NPT due to, it contains seven adsorption centers (4-N, 3-O and one S atom). Compound MPT comes after compound XPT in inhibition efficiency due to, it has six adsorption centers (4-N, One O and one S atom). Compound BPT is the least effective one due to; it has six adsorption centers (4-N, one O, one S atom and one Br atom). The Br-atom is withdrawing atom decreases the electron cloud on the molecule and hence decrease the % I.

### 4. Conclusions

- 1- The inhibition efficiency of the investigated phenylthiazole derivatives on corrosion of zinc in 0.2 M HCl solution increases by increasing the concentration of inhibitor and decreases with increasing temperature
- 2- Potentiodynamic polarization measurements show that the studied inhibitors act as mixed type inhibitors
- 3- The adsorption of the investigated inhibitors is found to obey Langmuir adsorption isotherm
- 4- The negative values of  $\Delta G^\circ_{ads}$  indicate spontaneous adsorption of the inhibitors on the zinc surface
- 5- EIS measurement reveals that the charge transfer resistance increases and the double layer capacitance decreases with increase in concentration of the inhibitors
- 6- The obtained results from electrochemical methods showed good agreement with that obtained from chemical method

### 5. References

- [1] G.W. Walther, Corros. Sci. 16 (1976) 573.
- [2] Lin Wang, Jian-XinPu, Hui-Chun Luo, Corros. Sci., 45 (2003) 677.
- [3] A. Abdel Nazeer, H. M. El-Abbasy, A.S. Fouda, Res. Chem. Intermed. 39 (2013) 921.
- [4] F. Bentiss, M. Bouanis, B. Mernari, M. Traisnel, H. Vezin, M. Lagrenee, Appl. Surf. Sci. 253 (2007) 3696.
- [5] M. A. Quraishi, A. Ishtiaque, S. A. Kumar, Mater. Chem. Phys. 112 (2008) 1035.
- [6] B. Tang, D. Li, F. Fu, Y. Xu, G. Yu, J. Zhang, Ind. Eng. Chem. Res. 51 (2012) 2615.
- [7] O. Olivares, N.V. Likhanova, B. Gomez, J. Navarrete, M.E. Llanos-Serrano, E. Arce, J.M. Hallen, Appl. Surf. Sci. 252 (2006) 2894
- [8] S. Trasatti, Electrochim. Acta 37 (1992) 2137
- [9] A. Popova, E. Sokolova, S. Raicheva, M. Christov, Corros. Sci. 45 (2003) 33
- [10] A. Abdel Nazeer, H. M. El-Abbasy, A. S. Fouda, J. Mater. Eng. Perform., 22 (2013) 2314.
- [11] R.W. Revie, Uhlig's Corrosion Handbook (Wiley, New York, 2000)
- [12] M.S. Abdel Aal, A.A. Abdel Wahab, A.El-Saied, Thermodynamic study of corrosion of zinc metal, Corrosion 37(10) (1981) 557.
- [13] L.Wang, J.X.Pu and H.C.Luo, (2003): Quantum mechanical calculations of amino pyrazole derivatives as corrosion inhibitors for zinc in acid chloride solution, Corros. Sci., 45, 677.
- [14] S.A. Odomelam, E.C. Ogoko, B.I.Ito, N.O. Eddy, Adsorption and Inhibitive Properties of Clarithromycin for the Corrosion of Zn in 0.01 to 0.05 M  $H_2SO_4$ , Portug. Electrochim.Acta, 2009, 27(1), p 57-68



- [15] Y.K.Agrawal, J.D.Talati, M.D.Shah, M.N.Desai, N.K.Shah, Schiff Bases of Ethylenediamine as Corrosion Inhibitors of Zinc in Sulphuric Acid Corros.Sci., 2004, 46, p 633- 651
- [16] M.S.Abdal-Aal,Z.A.Ahmed, M.S. Hassan Inhibiting and Accelerating Effects of some Quinolines on the Corrosion of Zinc and some Binary Zinc Alloys in HCl Solution, J. Appl.Electrochem., 1992, 22, p 1104-1109
- [17] The Effect of Aloe Vera Extract on Corrosion and Kinetics of Zinc in HCl Solution, Corros. Sci., 2010, 52(2), p 661-664
- [18] M. Abdallah, A.y. El-Etre, M.F. Moustafa, AmidopolyEthylamines as Corrosion Inhibitors for Zinc Dissolution in Different Acidic Electrolyte,Portuge. Electrochim.Acta, 2009, 27(5), p 615-630
- [19] M. Abdallah, Ethoxylate Fatty Alcohols as Corrosion Inhibitor for Dissolution of Zinc in Hydrochloric Acid. Corros. Sci., 2003, 45, p 2705-2716
- [20] E.E. Foad El-Sherbini, S.M. Abd El-Wahab, M. Deyab, Ethoxylated Fatty Acids as Inhibitors for the Corrosion of Zinc in Acid Media, Mater. Chem. Phys. 2005, 89, p183-191
- [21] M.N. Desai, J.D. Talati, N.K. Sheh, Schiff Bases of Ethylenediamine/ Triethylenetetramine with Benzaldehyde/Cinnamic Aldehyde/SalicylaldehydeAs Corrosion Inhibitors of Zinc in Sulphuric Acid, Anti-Corros. Meth.Mater., 55(1) (2008) 27-37
- [22] A.S. Fouda and L.H. Madkour, Inhibitive Action of Some Amines and Hydrazines Towards Corrosion of Zinc in Trichloroacetic Acid Solution, Bull. Soc. Chim. France, 1986, 5, p 745-749
- [23] A.S. Fouda, A.K. Mohamed, H.A. Mostafa and E.M. Hussein, A Study of the Inhibiting Action of Some Monosaccharides on the Corrosion of Zinc in HNO<sub>3</sub> J. Indian Chem. Soc., 1989, 66, p 417- 419
- [24] A.S. Fouda, L.H. Madkour, A.A.El-Shafei and S.A. Maksoud, Corrosion Inhibitors for Zinc in 2M HCl Solution, Korean Chem. Soc., 1995, 16(5), p 454-458
- [25] A.S. Fouda, M. Abdallah, S.T. Atwa and M.M. Salem, Tetrahydrocarbazole Derivatives as Corrosion Inhibitors for Zn in HCl Solution, Modern Applied Science, 2010, 4(12), p 41-55.
- [26] E.S. Lisac and S. Podbrscek, Non-toxic Organic Zinc Corrosion inhibitors in Hydrochloric Acid, J. Appl. Electrochem., 1994, 24, p 779-784
- [27] F. Bentiss, M. Lebrini and M. Lagrenee, Corros. Sci., 472 (2005) 915
- [28] M. Abdallah, Corros. Sci. 46 (2004) 1981.
- [29] I. Langmuir, J. Amer. Chem. Soc., 39 (1947) 1848.
- [30] E. Khamis. The Effect of Temperature on the Acidic Dissolution of Steel in the Presence of Inhibitors. Corrosion 46 (1990) 476.
- [31] Oguzie EE. [Corrosion inhibition of aluminium in acidic and alkaline media by Sansevieria trifasciata extract](#). Corros.Sci 49 (2007) 1527.
- [32] A.K. Singh, M.A. Quraishi, Effect of Cefazolin on the corrosion of mild steel in HCl solution, Corros. Sci., 52(2010)156
- [33] Y.A. El-Awady, A.I. Ahmed, Effect of temperature and inhibitors on the corrosion of aluminum in 2N HCl solution: a kinetic study. J. Ind. Chem. 24A (1985) 601.
- [34] A.S. Fouda, M.F. El-Sherbiny, M.M. Motawea. Corrosion inhibition of aluminum alloy in H<sub>3</sub>PO<sub>4</sub> solution using parathiazolidinone derivatives, Desalination and Water Treatment, 30 (2011) 1-10
- [35] E.S. Ferreira, C. Giacomelli, F.C. Gicomelli, A. Spinelli, Mater. Chem. Phys., 83(1), 129 (2004)
- [36] A. Popova, E. Sokolova, S. Raicheva, M. Christov, Corros sci., 45(2003) 33
- [37] E.E. Oguzie, CorrosSci, , 49, 1529 (2007).
- [38] J. Marsh "Advanced Organic Chemistry" 3rd ed., Wiley Eastern New Delhi, (1988).
- [39] G.K. Gomma, M.H. Wahdan. [Schiff bases as corrosion inhibitors for aluminum in hydrochloric acid solution](#). Mater.Chem. Phys. 39 (1995) 209.
- [40] S.S. Abd El-Rehim, M.A.M. Ibrahim, K.F. Khaled, 4-Aminoantipyrine as an inhibitor of mild steel corrosion in HCl solution, J. Appl. Electrochem.29 (1999) 593.
- [41] E.S. Ferreira, C. Giancomelli, F.C. Giacomelli and A. Spinelli, Mater. Chem. Phys., 83 (2004) 129.
- [42] O. Olivares, N.V. Likhanova, B. Gomez, J. Navarrete, M.E. Llanos-Serrano, E. Arce, J.M. Hallen, Appl. Surf. Sci., 252 (2006) 2894.



- [43] S.S. Abdel Rehim, H.H. Hassan, M.A. Amin, Appl. Surf. Sci. 187 (2002) 279.
- [44] O.E. Barcia, O.R. Mattos, N. Pebere, B. Tribollet, J. Electrochem. Soc. 140 (1993) 2825.
- [45] C. Deslouis, B. Tribollet, G. Mengoli, M.M. Musiani, J. Appl. Electrochem. 18 (1988) 374.
- [46] X. Wu, H. Ma, S. Chen, Z. Xu, A. Sui, J. Electrochem. Soc. 146 (1999) 1847.
- [47] E. McCafferty, N. Hackerman, J. Electrochem. Soc., 119 (1972) 146.
- [48] S. Muralidharan, K.L.N. Phani, S. Pitchumani, S. Ravichandran, J. Electrochem. Soc., 42 (1995) 1478
- [48] M. Bethencourt, F. J. Botana, J. J. Calvino, M. Marcos, Lanthanide compounds as environmentally-friendly corrosion inhibitors of aluminium alloys: A review. Corros. Sci. 40 (1998) 1803-1819.
- [49] Gamry Instruments. Echem Analyst Manual, 2003.
- [50] R.W. Bosch, W.F. Bogaerts, Corrosion 52 (1996) 204.
- [51] R.W. Bosch. J. Hubrecht. W.F. Bogaerts. B.C. Syrret, Corrosion 57 (2001) 60-70
- [52] 34. A.K. Mohamed, T.H. Rakha and M.N. Moussa, Bull. Soc. Chem. Fr., **127**, 375 (1990).
- [53] IshtiaqueAhamad, Rajendra Prasad and M.A. Quraishi, Corros. Sci., 52 (2010) 3033.
- [54] L.I. Antropov, Corros. Sci., 7 (1967)

Table 1: Effect of inhibitors concentrations on the inhibition efficiency of zinc in 0.2 M HCl solution from weight-loss method at 30 °C

% I				
[Inhibitor]	NPT	XPT	MPT	BPT
M				
$1 \times 10^{-6}$	79.9	66.6	62.2	60.2
$5 \times 10^{-6}$	83.9	79	71.9	68.9
$1 \times 10^{-5}$	89.2	81	74.3	72.9
$3 \times 10^{-5}$	92.8	86.6	85.3	79.1
$5 \times 10^{-5}$	96.7	91.9	86.1	83.9
$7 \times 10^{-5}$	97.5	90.9	89.1	86.8

Table 2: Slopes of Langmuir isotherm lines, adsorption equilibrium constant of the investigated compounds ( $K_{ads}$ ) and free energy of adsorption ( $\Delta G_{ads}^{\circ}$ ) of inhibitors for zinc in 0.2 M HCl at 30°C

Langmuir isotherm			
Inhibitors	Slope	$K_{ads} \times 10^{-5}$	$-\Delta G_{ads}^{\circ}$
		$M^{-1}$	$kJ mol^{-1}$
NPT	1.024	3.4	39.7
XPT	1.038	2.6	35.5
MPT	1.084	2.2	31.2
BPT	1.012	1.5	29.5





Table 3: Corrosion parameters of zinc electrode in 0.2 M HCl solution containing different concentrations of the investigated phenylthiazole derivatives

Comp.	Conc., M	-E <sub>corr.</sub> mV vs SCE	i <sub>corr.</sub> , mA cm <sup>-2</sup>	β <sub>c</sub> mV dec <sup>-1</sup>	β <sub>a</sub> mV dec <sup>-1</sup>	θ	% I
	Blank	987	22.2	308	157	-	-
NPT	1x10 <sup>-6</sup>	978	6.45	282	158	0.709	70.9
	5x10 <sup>-6</sup>	977	5.03	283	148	0.773	77.3
	1x10 <sup>-5</sup>	965	4.62	278	151	0.792	79.2
	3x10 <sup>-5</sup>	955	3.17	271	147	0.857	85.7
	5x10 <sup>-5</sup>	965	2.7	268	137	0.878	87.8
	7x10 <sup>-5</sup>	964	1.08	265	125	0.951	95.1
XPT	1x10 <sup>-6</sup>	980	7.9	255	179	0.644	64.4
	5x10 <sup>-6</sup>	968	6.61	250	166	0.702	70.2
	1x10 <sup>-5</sup>	966	6.1	243	143	0.725	72.5
	3x10 <sup>-5</sup>	967	4.85	214	142	0.782	78.2
	5x10 <sup>-5</sup>	969	3.62	230	138	0.837	83.7
	7x10 <sup>-5</sup>	959	1.69	228	129	0.924	92.4
MPT	1x10 <sup>-6</sup>	989	8.24	286	146	0.629	62.9
	5x10 <sup>-6</sup>	973	6.59	281	151	0.703	70.3
	1x10 <sup>-5</sup>	972	5.75	265	146	0.741	74.1
	3x10 <sup>-5</sup>	987	4.25	261	144	0.809	80.9
	5x10 <sup>-5</sup>	965	2.98	245	131	0.866	86.6
	7x10 <sup>-5</sup>	963	2.27	231	118	0.898	89.8
BPT	1x10 <sup>-6</sup>	978	10.7	264	166	0.518	51.8
	5x10 <sup>-6</sup>	977	8.06	252	151	0.637	63.7
	1x10 <sup>-5</sup>	971	6.25	241	147	0.718	71.8
	3x10 <sup>-5</sup>	969	4.72	234	142	0.787	78.7
	5x10 <sup>-5</sup>	978	3.3	227	146	0.851	85.1
	7x10 <sup>-5</sup>	982	2.87	229	126	0.871	87.1



Table 4: Effect of inhibitors concentrations on the activation energy, activation enthalpy and activation entropy of zinc dissolution in 0.2 M HCl

	Conc., M	Compounds			
		BPT	MPT	XPT	NPT
$\Delta E^*$ , kJ mol <sup>-1</sup>	Blank	45.3			
	1×10 <sup>-5</sup>	31.4	35.7	38.2	41.8
	3×10 <sup>-5</sup>	30.7	33.4	36.5	38.4
	5×10 <sup>-5</sup>	29.2	31.3	35.1	36.3
	7×10 <sup>-5</sup>	27.8	30.6	33.2	34.8
$\Delta H^*$ , kJ mol <sup>-1</sup>	Blank	21.1			
	1×10 <sup>-5</sup>	56.2	46.8	41.4	23.8
	3×10 <sup>-5</sup>	59.5	48.3	41.9	21.7
	5×10 <sup>-5</sup>	63.0	52.5	49.3	16.3
	7×10 <sup>-5</sup>	64.1	53.4	50.2	14.1
$\Delta S^*$ , J mol <sup>-1</sup> K <sup>-1</sup>	Blank	51.2			
	1×10 <sup>-5</sup>	14.9	22.0	34.2	11.7
	3×10 <sup>-5</sup>	13.4	17.5	31.4	10.2
	5×10 <sup>-5</sup>	8.9	10.7	17.6	8.6
	7×10 <sup>-5</sup>	7.6	8.2	13.4	7.1



Table 5: Electrochemical kinetic parameters obtained by EIS technique for the corrosion of zinc in 0.2 M HCl solution in the absence and presence of different concentrations of the studied phenylthiazole derivatives at 30°C

Comp.	Conc., M	$C_{dl}$ $\mu F/cm^2$	$R_{ct}$ $\Omega cm^2$	$\theta$	% I
BPT	Blank	125.9	12.35	-	-
	$1 \times 10^{-5}$	118.2	53.83	0.771	77.1
	$3 \times 10^{-5}$	88.61	73.35	0.832	83.2
	$5 \times 10^{-5}$	76.6	92.7	0.867	86.7
	$7 \times 10^{-5}$	71.36	110.6	0.888	88.8
MPT	$1 \times 10^{-5}$	111.4	59.6	0.792	79.2
	$3 \times 10^{-5}$	95.66	82.1	0.849	84.9
	$5 \times 10^{-5}$	81.56	100.8	0.877	87.7
	$7 \times 10^{-5}$	73.5	119.7	0.896	89.6
XPT	$1 \times 10^{-5}$	106.1	66.1	0.813	81.3
	$3 \times 10^{-5}$	92.23	91.9	0.865	86.5
	$5 \times 10^{-5}$	70.63	108.5	0.886	88.6
	$7 \times 10^{-5}$	66.26	125.2	0.901	90.1
NPT	$1 \times 10^{-5}$	101.7	72.77	0.830	83.0
	$3 \times 10^{-5}$	75.42	111.5	0.889	88.9
	$5 \times 10^{-5}$	67.22	124.7	0.900	90.0
	$7 \times 10^{-5}$	61.77	148.7	0.917	91.7



Table 6: Electrochemical kinetic parameters obtained by EFM for zinc in 0.2 M HCl solution, in the absence and presence of different concentration of the studied phenylthiazole derivatives at 30°C

Comp.	Conc., M	$i_{corr}$ $\text{mA cm}^{-2}$	$\beta_a$ $\text{mV dec}^{-1}$	$\beta_c$ $\text{mV dec}^{-1}$	CF-2	CF-3	$\theta$	% I
NPT	Blank	63.1	79	165	1.93	3.09	-	-
	$1 \times 10^{-5}$	17.5	85	179	1.89	2.89	0.723	72.3
	$3 \times 10^{-5}$	11.2	89	188	1.96	3.05	0.823	82.3
	$5 \times 10^{-5}$	7.4	91	193	1.92	2.87	0.883	88.3
	$7 \times 10^{-5}$	3.7	102	199	1.98	3.01	0.941	94.1
XPT	$1 \times 10^{-5}$	20.1	87	170	1.92	2.85	0.681	68.1
	$3 \times 10^{-5}$	14.3	92	181	1.84	2.92	0.773	77.3
	$5 \times 10^{-5}$	10.1	99	189	1.91	3.01	0.839	83.9
	$7 \times 10^{-5}$	6.3	107	196	2.02	2.95	0.901	90.1
MPT	$1 \times 10^{-5}$	21.7	94	175	1.92	2.94	0.656	65.6
	$3 \times 10^{-5}$	15.8	98	184	2.02	3.03	0.749	74.9
	$5 \times 10^{-5}$	11.2	109	192	1.87	2.88	0.823	82.3
	$7 \times 10^{-5}$	6.89	118	207	1.94	2.94	0.891	89.1
BPT	$1 \times 10^{-5}$	23.4	99	180	1.86	2.89	0.629	62.9
	$3 \times 10^{-5}$	17.5	108	187	1.78	2.78	0.723	72.3
	$5 \times 10^{-5}$	12.3	112	198	1.96	3.06	0.805	80.5
	$7 \times 10^{-5}$	8.6	122	218	2.01	3.03	0.864	86.4

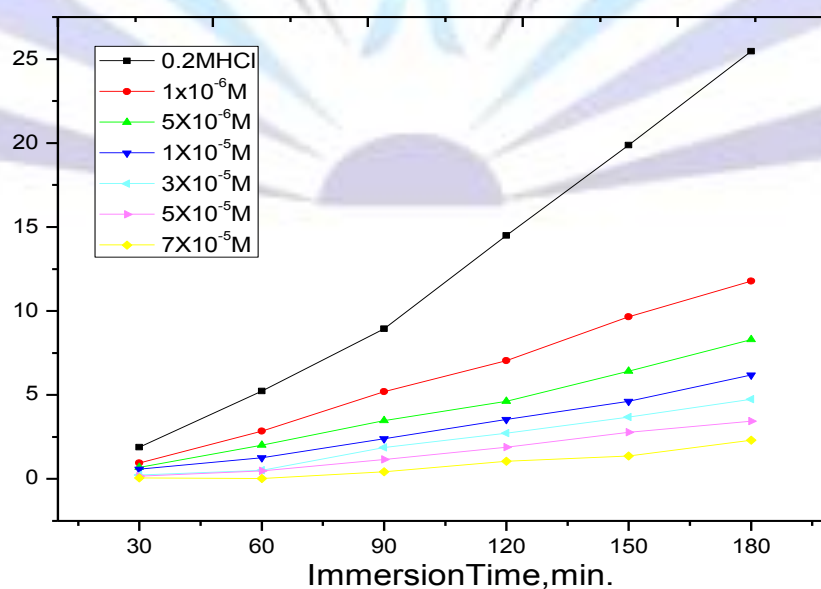


Figure (1) Weight loss-time curves for zinc dissolution in 0.2 M HCl in absence and presence of different concentrations of NPT at 30°C

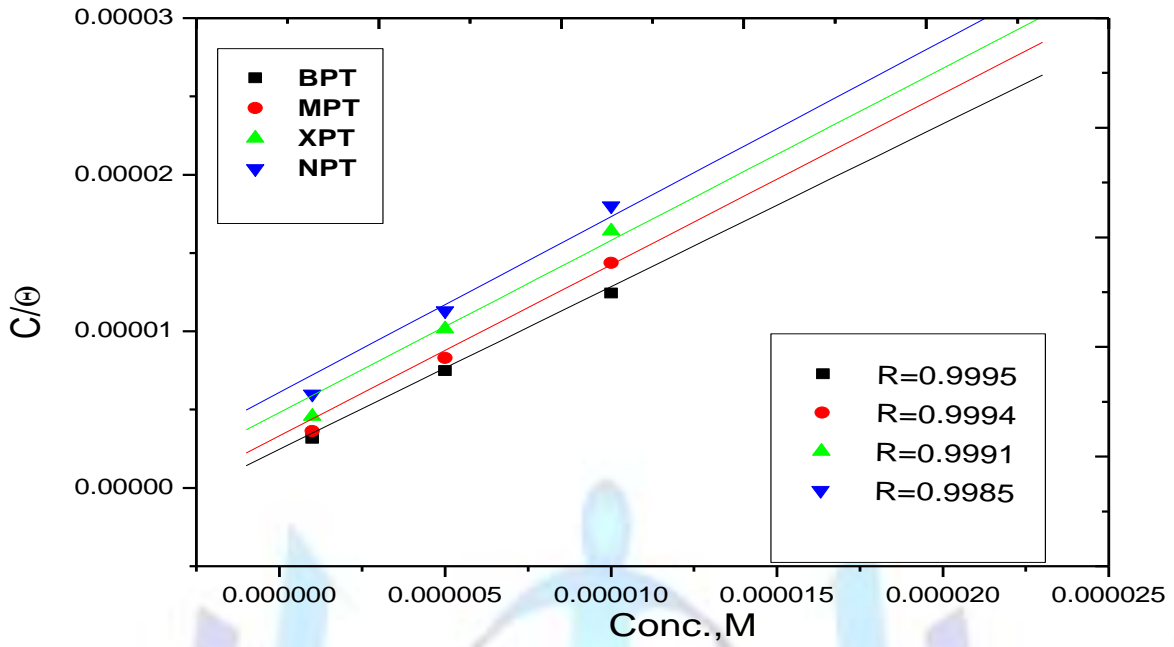


Figure (2): Langmuir adsorption isotherm plotted as  $(C/\theta)$  vs concentration of inhibitors for the corrosion of Zn in 0.2 M HCl at 30°C

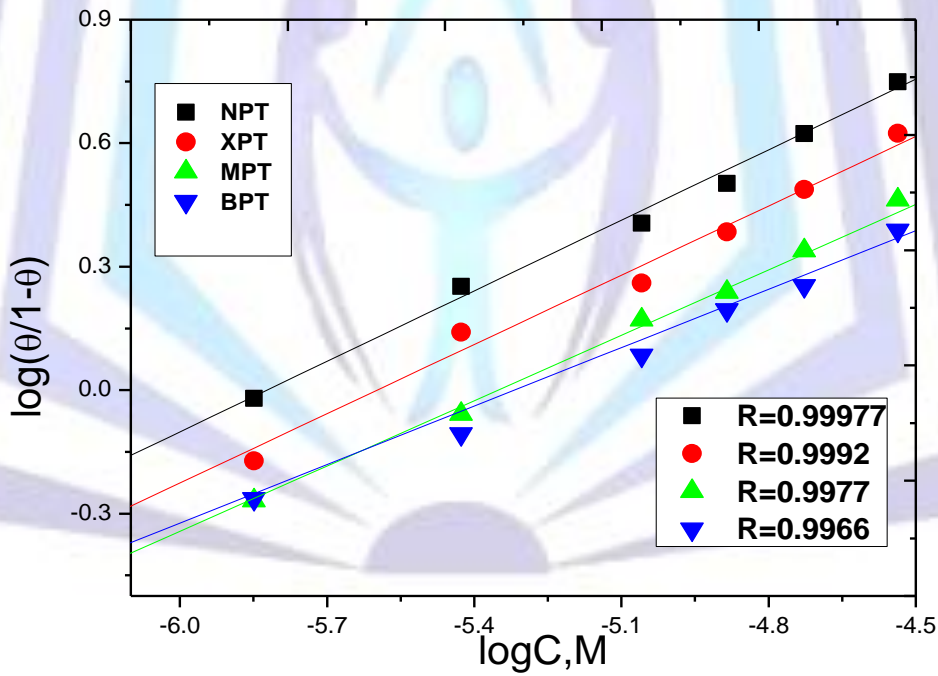


Figure (3): El-Awady model plotted as  $\log(\theta/(1-\theta))$  vs  $\log C$  of inhibitors for corrosion of Zn in 0.2 M HCl at 30°C

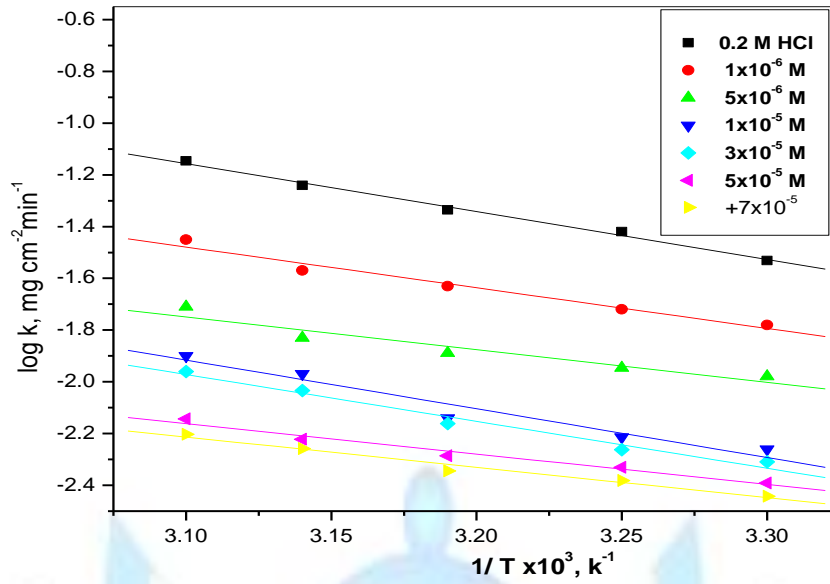


Figure (4) Arrhenius plots (log k vs. 1/T) for Zn in 0.2M HCl in the absence and presence of different concentrations of NPT

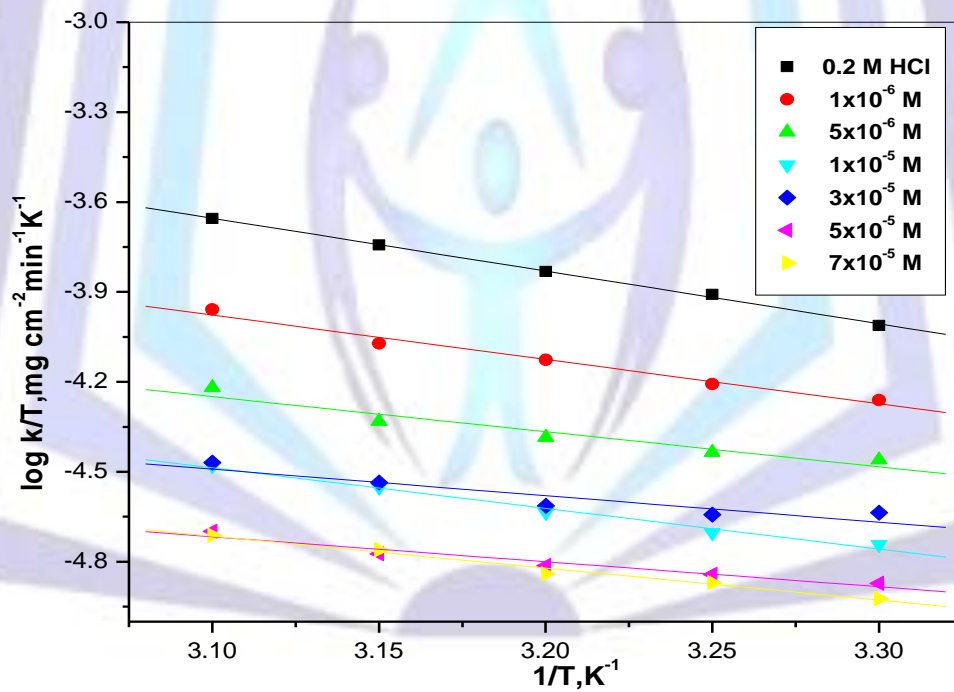


Figure (5): Arrhenius plots (log k/T vs 1/T) for Zn in 0.2 M HCl in the absence and presence of different concentrations of NPT

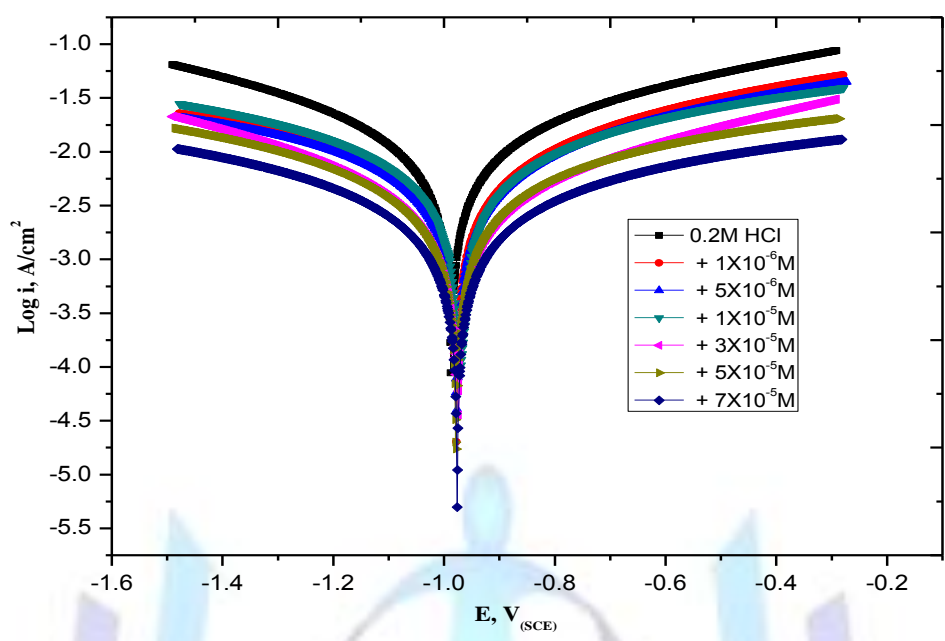


Figure (6): Potentiodynamic polarization curves for the corrosion of zinc in 0.2 M HCl solution in the absence and presence of different concentrations of BPT at 30°C

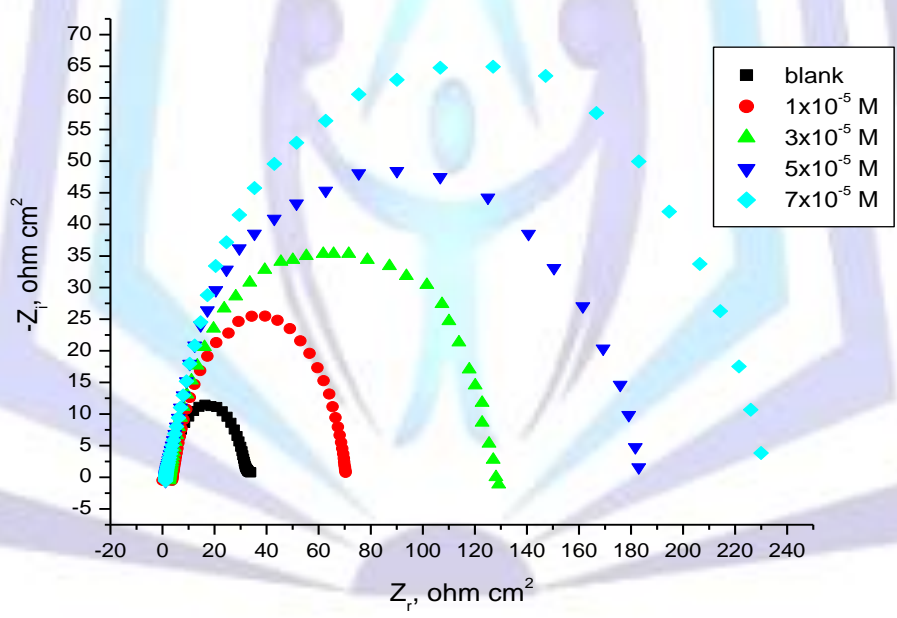


Figure (7): Nyquist plots recorded for zinc in 0.2M HCl in the absence and presence of different concentrations of BPT at 30°C

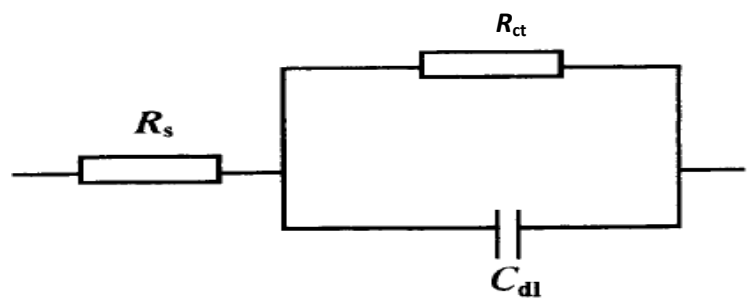


Figure (8): The equivalent circuit model.

